Short communication

Towards real-time (milliseconds) parameter estimation of lithium-ion batteries using reformulated physics-based models

Vijayasekaran Boovaragavan [1], S. Harinipriya [2], Venkat R. Subramanian [*]

Department of Chemical Engineering, Tennessee Technological University, Cookeville, TN 38505, United States

ABSTRACT

In this paper, transport and kinetic parameters of lithium-ion batteries are estimated using a rigorous porous electrode theory based model. The rigorous model used in this investigation is reformulated using advanced mathematical techniques. Since batteries and other electrochemical devices are used in hybrid environments, which include devices with time constants less than a second (like supercapacitor), we need to develop parameter estimation codes with computation time less than a second or a few milliseconds. In this investigation, the computation time for parameter estimation measures between 100 and 300 ms since a reformulated battery model is devised especially for these purposes. Obtaining the numerical solution for battery model equations is very difficult towards the end of discharge and is usually neglected for parameter estimation purposes. However, in this paper the estimation takes into account the entire discharge data ranging from an initial potential of 4.2 V to a cut-off potential of 2.5 V. It is found from this investigation that the reformulated lithium-ion battery model is efficient and accurate in estimating parameters.

© 2008 Elsevier B.V. All rights reserved.

1. Introduction

Several investigators have analyzed various rigorous models for lithium-ion batteries [1–12] based on the porous electrode theory coupled with concentration solution theory and modified Ohm's law. There are some important advances in these models in recent years like the thermal modeling of lithium-ion batteries [5] and modeling capacity fade mechanism in lithium-ion batteries [8]. The governing equations in these models include ten nonlinear, coupled and multidimensional partial differential equations (in the spatial directions x, r and t) that are needed to be solved simultaneously in time along with some highly nonlinear algebraic expressions for transport and kinetic parameters. Rigorous lithium-ion battery models need any where from several seconds to minutes to simulate a discharge curve depending on the computer, solver, etc. This computational difficulty in using rigorous battery models is due to the large number of equations that result from finite difference reformulation of battery models. Table 1 shows the total number of differential-algebraic equations (DAEs) needed for the rigorous model and the computation time required when the model

equations are solved for one charge or discharge curve and for one complete cycle. All the simulations in this work are based on a PC with 2.5 GHz processor and 2 GB RAM. Rigorous version of the model is not ideal due to the requirement of sufficient computational resources. Whereas, the reformulated efficient model could eventually in future run in a microprocessor to estimate parameters in a few milliseconds.

Until recently [13], there were no significant efforts for estimating parameters using the rigorous battery model because of computational constraints. There are several mathematical investigations for rapid solution of complicated model equations [14–22]. A more detailed article that presents the complete mathematical theory for an effective approach to simulate physics-based lithium-ion battery models in real-time (milliseconds) is under the process of publication [23]. Parameter estimation helps in calculating capacity fade and life time of the battery. However, empirical models or single particle model cannot help in estimating accurate parameter values. The capacity fade or the state-of-health information obtained using these parameters will not guarantee successful prediction for applications like hybrid vehicles, satellites or military applications. Also, it is to be noted that the batteries and other electrochemical devices are now-a-days emerging as a promising candidate for hybrid power systems. Since in a hybrid environment, there are devices like the supercapacitor with time constant less than a second, we also need to have a battery model that can be simulated in few milliseconds. To this point, this investigation and our future efforts on lithium-ion battery models are

---

* Corresponding author. Tel.: +1 931 372 3494; fax: +1 931 372 6352.
E-mail address: vsubramanian@tntech.edu (V.R. Subramanian).
[1] Oronzio de Nora Industrial Electrochemistry Fellow of The Electrochemical Society.
[2] Present address: Scientist, CRL, Laird Technologies, Bangalore 560066, India.

Nomenclature

a_i	specific surface area of electrode i ($i = p, n$) (m^2 m^{-3})
brugg$_i$	Bruggman coefficient of region i ($i = p, s, n$)
c	electrolyte concentration (mol m^{-3})
c_0	initial electrolyte concentration (mol m^{-3})
$c_{s,i}$	concentration of lithium ions in the intercalation particle of electrode i ($i = p, n$) (mol m^{-3})
$c_{s,i,0}$	initial concentration of lithium ions in the intercalation particle of electrode i ($i = p, n$) (mol m^{-3})
$c_{s,i,\max}$	maximum concentration of lithium ions in the intercalation particle of electrode i ($i = p, n$) (mol m^{-3})
D	electrolyte diffusion coefficient (m^2 s^{-1})
$D_{s,i}$	lithium ion diffusion coefficient in the intercalation particle of electrode i ($i = p, n$) (m^2 s^{-1})
F	Faraday's constant (C mol^{-1})
i_1	solid-phase current density (A m^{-2})
i_2	solution phase current density (A m^{-2})
$i_{s,0}$	exchange current density for the solvent reduction reaction (A m^{-2})
I	applied current density (A cm^{-2})
j_i	wall flux of Li$^+$ on the intercalation particle of electrode i ($i = n, p$) (mol m^{-2} s^{-1})
j_s	solvent reduction current density (mol m^{-2} s^{-1})
k_i	intercalation/deintercalation reaction rate constant of electrode i ($i = p, n$) (mol (mol m^{-3})$^{-1.5}$)
l_i	thickness of region i ($i = p, s, n$) (m)
M_s	molar weight of the solvent reaction product (g mol^{-1})
n	negative electrode
p	positive electrode
r	radial coordinate (m)
R	universal gas constant (J (mol^{-1} K^{-1}))
R_i	radius of the intercalation particle of electrode i ($i = p, n$) (m)
R_{SEI}	initial SEI layer resistance at the negative electrode (Ω m^{-2})
s	separator
t_+	Li$^+$ transference number in the electrolyte
T	absolute temperature (K)
U_i	open circuit potential of electrode i ($i = p, n$) (V)
U_s	standard potential of the solvent reduction reaction (V)
x	spatial coordinate (m)

Greek symbols

Φ_1	solid-phase potential (V)
Φ_2	electrolyte phase potential (V)
δ	thickness of the solvent reduction product film (m)
δ_0	initial thickness of the solvent reduction product film (m)
ε_i	porosity of region i ($i = p, s, n$)
$\varepsilon_{f,i}$	volume fraction of fillers of electrode i ($i = p, n$)
κ	ionic conductivity of the electrolyte (S m^{-1})
$\kappa_{eff,i}$	effective ionic conductivity of the electrolyte in region i ($i = p, s, n$) (S m^{-1})
θ_i	dimensionless concentration of lithium ions in the intercalation particle of electrode i ($\theta_i = c_{s,i}/c_{s,i,\max}$)
ρ_s	density of the solvent reduction product film (g m^{-3})
σ_i	electronic conductivity of the solid phase of electrode i ($i = p, n$) (S m^{-1})
$\sigma_{eff,i}$	effective electronic conductivity of the solid phase of electrode i ($i = p, n$) (S m^{-1})

Table 1
Properties of the rigorous porous electrode model and the reformulated porous electrode model

Computation details	Rigorous model	Reformulated model
Number of equations for charge or discharge curve	4800 DAEs	49 DAEs
Computation time for charge or discharge curve	1–2 min	15–45 ms
Estimated time for one complete cycle	5–10 min	75–100 ms

focused on real-time simulation, parameter estimation, dynamic optimization, and on-line control and monitoring of batteries that can work with CPU time less than a second.

Santhanagopalan et al. [13] used the Levenberg-Marquardt method to estimate parameters using rigorous lithium-ion battery models. Two different models, the single particle model and the rigorous porous electrode model, were used to estimate parameters at four different rates. Confidence intervals for the estimated parameters were reported, however, the computational time involved in this investigation was not highlighted; perhaps because of the necessity to do expensive, cumbersome and time-consuming simulation while using the porous electrode model. The authors [19,20] have studied the validity of estimating the solid-phase diffusion coefficient of a lithium intercalation electrode from impedance measurement by a modified electrochemical impedance spectroscopy method. This paper showed that single particle models are not accurate and are hence not useful.

To overcome this drawback, we have devised a novel reformulated lithium-ion battery model that can help in simulating battery behavior in real-time (milliseconds) [21]. This novel reformulated battery model has been used in this article for parameter estimation. The model used in this investigation is based on the same porous electrode model for the lithium-ion cell that is used in ref. [13]. However, it is found that the computation time required for the parameter estimation is only on the order of a few milliseconds in this investigation. Table 1 also shows the number of DAEs required in solving the reformulated battery model and the computation time associated with it while solving the model for one charge or discharge curve and for one complete cycle. The reformulated lithium-ion battery model is efficient and accurate for parameter estimation. It is also important to note that with the use of reformulated lithium-ion battery model the numerical Jacobian calculation is good enough for accurate parameter estimation. Thus, this investigation enables the possibility for real-time estimation of parameters that can be useful in predicting the capacity fade and life time of the lithium-ion batteries. It should be noted that the model reformulation provides predictive models and are as good as original model for a wide range of operating conditions. It is significantly different from proper orthogonal decomposition approach which is based on curve fitting eigen values and eigen vectors to produce reduced order models from rigorous numerical simulation [24–26].

2. Reformulated lithium-ion battery model

The existing rigorous physics-based lithium-ion battery model [5] has multiple partial differential equations in multiple domains. The lithium-ion battery model involves two independent spatial variables (radial direction, r and linear direction, x) and a time variable, t. There are four dependent variables, namely electrolyte concentration (c), electrolyte potential (Φ_2), solid-phase concentration (c_s) and solid-phase potential (Φ_1) for each of the two porous electrodes. The two dependent variables for separator are electrolyte concentration (c) and electrolyte potential (Φ_2). The governing equations for all these variables are shown in Table 2

Table 2
Governing equations for a lithium-ion cell based on the porous electrode theory

Region	Eq. no.	Governing equations	Boundary conditions
Cathode	(1)	$\varepsilon_p \frac{\partial c}{\partial t} = D_{eff,p} \frac{\partial^2 c}{\partial x^2} + a_p(1-t_+)j_p$ initial condition $c\|_{t=0} = c_0$	$-D_{eff,p} \frac{\partial c}{\partial x}\big\|_{x=0} = 0$ & $-D_{eff,p} \frac{\partial c}{\partial x}\big\|_{x=l_p,-} = -D_{eff,s} \frac{\partial c}{\partial x}\big\|_{x=l_p,+}$
	(2)	$-\sigma_{eff,p} \frac{\partial \Phi_1}{\partial x} - \kappa_{eff,p} \frac{\partial \Phi_2}{\partial x} + \frac{2\kappa_{eff,p}RT}{F}(1-t_+) \frac{\partial \ln c}{\partial x} = I$	$-\kappa_{eff,p} \frac{\partial \Phi_2}{\partial x}\big\|_{x=0} = 0$ & $-\kappa_{eff,p} \frac{\partial \Phi_2}{\partial x}\big\|_{x=l_p,-} = -\kappa_{eff,s} \frac{\partial \Phi_2}{\partial x}\big\|_{x=l_p,+}$
	(3)	$\sigma_{eff,p} \frac{\partial^2 \Phi_1}{\partial x^2} = a_p F j_p$	$\frac{\partial \Phi_1}{\partial x}\big\|_{x=0} = -\frac{I}{\sigma_{eff,p}}$ & $-\sigma_{eff,p} \frac{\partial \Phi_1}{\partial x}\big\|_{x=l_p} = 0$
	(4)	$\frac{\partial c_s}{\partial t} = \frac{D_{s,p}}{r^2} \frac{\partial}{\partial r}\left(r^2 \frac{\partial c_s}{\partial r}\right)$ initial condition $c_s\|_{t=0} = 0.5c_{s,max,p}$	$\frac{\partial c_s}{\partial r}\big\|_{r=0} = 0$ & $j_p = -D_{s,p} \frac{\partial c_s}{\partial r}\big\|_{r=R_p}$
Separator	(5)	$\varepsilon_s \frac{\partial c}{\partial t} = D_{eff,s} \frac{\partial^2 c}{\partial x^2}$	$-D_{eff,p} \frac{\partial c}{\partial x}\big\|_{x=l_p,-} = -D_{eff,s} \frac{\partial c}{\partial x}\big\|_{x=l_p,+}$ & $-D_{eff,s} \frac{\partial c}{\partial x}\big\|_{x=l_p+l_s,-} = -D_{eff,n} \frac{\partial c}{\partial x}\big\|_{x=l_p+l_s,+}$
	(6)	$I = -\kappa_{eff,s} \frac{\partial \Phi_2}{\partial x} + \frac{2\kappa_{eff,s}RT}{F}(1-t_+) \frac{\partial \ln c}{\partial x}$	$-\kappa_{eff,p} \frac{\partial \Phi_2}{\partial x}\big\|_{x=l_p,-} = -\kappa_{eff,s} \frac{\partial \Phi_2}{\partial x}\big\|_{x=l_p,+}$ & $-\kappa_{eff,s} \frac{\partial \Phi_2}{\partial x}\big\|_{x=l_p+l_s,-} = -\kappa_{eff,n} \frac{\partial \Phi_2}{\partial x}\big\|_{x=l_p+l_s,+}$
Anode	(7)	$\varepsilon_n \frac{\partial c}{\partial t} = D_{eff,n} \frac{\partial^2 c}{\partial x^2} + a_n(1-t_+)j_n$ initial condition $c\|_{t=0} = c_0$	$-D_{eff,s} \frac{\partial c}{\partial x}\big\|_{x=l_p+l_s,-} = -D_{eff,n} \frac{\partial c}{\partial x}\big\|_{x=l_p+l_s,+}$ & $D_{eff,n} \frac{\partial c}{\partial x}\big\|_{x=l_p+l_s+l_n} = 0$
	(8)	$-\sigma_{eff,n} \frac{\partial \Phi_1}{\partial x} - \kappa_{eff,n} \frac{\partial \Phi_2}{\partial x} + \frac{2\kappa_{eff,n}RT}{F}(1-t_+) \frac{\partial \ln c}{\partial x} = I$	$-\kappa_{eff,s} \frac{\partial \Phi_2}{\partial x}\big\|_{x=l_p+l_s,-} = -\kappa_{eff,n} \frac{\partial \Phi_2}{\partial x}\big\|_{x=l_p+l_s,+}$ & $\Phi_2\big\|_{x=l_p+l_s+l_n} = 0$
	(9)	$\sigma_{eff,n} \frac{\partial^2 \Phi_1}{\partial x^2} = a_n F j_n$	$-\sigma_{eff,n} \frac{\partial \Phi_1}{\partial x}\big\|_{x=l_p+l_s} = 0$ & $\frac{\partial \Phi_1}{\partial x}\big\|_{x=l_p+l_s+l_n} = -\frac{I}{\sigma_{eff,n}}$
	(10)	$\frac{\partial c_s}{\partial t} = \frac{D_{s,n}}{r^2} \frac{\partial}{\partial r}\left(r^2 \frac{\partial c_s}{\partial r}\right)$ initial condition $c_s\|_{t=0} = 0.85c_{s,max,n}$	$\frac{\partial c_s}{\partial r}\big\|_{r=0} = 0$ & $j_n = -D_{s,n} \frac{\partial c_s}{\partial r}\big\|_{r=R_n}$

Table 3
Expressions used in the lithium-ion battery model given by Table 1

$\kappa_{eff,i} = \varepsilon_i^{brugg_i}(4.1253 \times 10^{-2} + 5.007 \times 10^{-4}c - 4.7212 \times 10^{-7}c^2 + 1.5094 \times 10^{-10}c^3 - 1.6018 \times 10^{-14}c^4), \quad i = p, s, n$

$\sigma_{eff,i} = \sigma_i(1 - \varepsilon_i - \varepsilon_{f,i}), \quad i = p, n$

$D_{eff,i} = D\varepsilon_i^{brugg_i}, \quad i = p, s, n$

$a_i = \frac{3}{R_i}(1 - \varepsilon_i - \varepsilon_{f,i}), \quad i = p, n$

$j_p = 2k_p(c_{s,max,p} - c_{s,p}\|_{r=R_p})^{0.5} c_{s,p}\|_{r=R_p}^{0.5} c^{0.5} \sinh\left[\frac{0.5F}{RT}(\Phi_1 - \Phi_2 - U_p)\right]$

$U_p = \dfrac{-4.656 + 88.669\theta_p^2 - 401.119\theta_p^4 + 342.909\theta_p^6 - 462.471\theta_p^8 + 433.434\theta_p^{10}}{-1.0 + 18.933\theta_p^2 - 79.532\theta_p^4 + 37.311\theta_p^6 - 73.083\theta_p^8 + 95.96\theta_p^{10}}$

where : $\theta_p = c_{s,p}\big\|_{r=R_p} / c_{s,p,max}$

$j_n = 2k_n(c_{s,max,n} - c_{s,n}\big\|_{r=R_n})^{0.5} c_{s,n}\big\|_{r=R_n}^{0.5} c^{0.5} \sinh\left[\frac{0.5F}{RT}(\Phi_1 - \Phi_2 - U_n + FR_{SEI}j_n)\right]$

$U_n = 0.7222 + 0.1387\theta_n + 0.029\theta_n^{0.5} - \frac{0.0172}{\theta_n} + \frac{0.0019}{\theta_n^{1.5}} + 0.2808 \exp(0.90 - 15\theta_n) - 0.7984 \exp(0.4465\theta_n - 0.4108)$

where : $\theta_n = c_{s,n}\big\|_{r=R_n} / c_{s,n,max}$

and the expressions used for the electrochemical reaction kinetics and other transport properties can be found in Table 3. A review on available simulation techniques for solving such a complicated lithium-ion battery model was made earlier [9].

These model equations are usually discretized using finite differences in the spatial coordinates resulting in 4800 DAEs. When 4800 DAEs are needed to solve for a simulation of the model equations, the Jacobian for parameter estimation will add some thousands more DAEs. Together, we will have several thousands of DAEs to estimate one parameter. If we go for instead to predict more than one parameter, then the number of equations to be solved will keep increasing proportionally. Obviously, this situation is not ideal for emerging applications like hybrid power systems, on-line control and monitoring of batteries and other electrochemical power sources. It will take several hours or days to estimate parameters in the model equations.

The authors have worked extensively in model reformulation and have already published the details on the reformulation of lithium-ion battery model [21,22]. This can enable a simulation of porous model equations in 15–45 ms as against 90–120 s for a similar simulation using rigorous porous model equations. This is achieved by efficiently combining the advanced mathematical approximation techniques with the actual physics of the electrochemical system under consideration. Now, the number of DAEs needed for a simulation is only 29–49.

3. Parameter estimation

A list of fixed parameters for the model equations are given in Table 4, and the following parameters are estimated (1) the solid-phase diffusion coefficient in negative electrode, $D_{s,n}$ (2) the electrolyte diffusion coefficient, D (3) the electrochemical rate constant in positive electrode, k_p and (4) the electrochemical rate constant in negative electrode, k_n. The unknown parameters are estimated using Gauss-Newton method from the synthetic experimental data obtained using computer generated random numbers. Here, the synthetic data is obtained by distributing 5% randomness error to the actual model predicted discharge data by considering 102 data points. The expression used to generate experimental values using Maple's random number generator is,

$$Z_{experimental} = Z_{analytical}[0.95 + 0.01(\text{Random number between 0 and 10})].$$

The synthetic experimental data are then provided to the parameter estimation algorithm along with appropriate initial guesses. The following steps are involved in the estimation of parameters: (i) start with good initial guesses for parameters, $\mathbf{k}^{(0)}$ (ii) compute the state and sensitivity variables of the model at each data point and set up the vector with experimental values $\mathbf{Y}_{exp}$, predicted values $\mathbf{Y}_{pre}$ and the Jacobian matrix $\mathbf{J}$ (iii) the correction fac-

Table 4
Parameters used for the simulation (LiCoO$_2$ and LiC$_6$ system)

Symbol	Unit	Positive electrode	Separator	Negative electrode
σ_i	S m^{-1}	100		100
$\varepsilon_{f,i}$		0.025		0.0326
ε_i		0.385	0.724	0.485
Brugg			4	
$D_{s,i}$	m^2 s^{-1}	1.0×10^{-14}		3.9×10^{-14}
D	m^2 s^{-1}		7.5×10^{-10}	
k_i	mol $(s^{-1}\,m^{-2})[(mol\,m^{-3})^{1+\alpha a,i}]^{-1}$	2.334×10^{-11}		5.0307×10^{-11}
$c_{s,i,max}$	mol m^{-3}	51,554		30,555
$c_{s,i0}$	mol m^{-3}	$0.4955 \times 51{,}554$		$0.8551 \times 30{,}555$
C_0	mol m^{-3}		1000	
R_p	m	2.0×10^{-6}		2.0×10^{-6}
l_i	m	80×10^{-6}	25×10^{-6}	88×10^{-6}
R_{SEI}	Ω m^2			0.0
T_+			0.363	
F	C mol^{-1}		96,487	
R	J (mol^{-1} K^{-1})		8.314	
T	K		298.15	

tor is obtained by using the expression, $\Delta \mathbf{k} = (\mathbf{J}^T\mathbf{J})^{-1}\mathbf{J}^T(\mathbf{Y}_{exp} - \mathbf{Y}_{pre})$ (iv) using this, the updated parameter values can be obtained as $\mathbf{k}^{(i+1)} = \mathbf{k}^{(i)} + r\Delta\mathbf{k}^{(i)}$, the predicted parameter for the next iteration is $\mathbf{k}^{(i+1)}$, r is the correction factor. Steps (ii) to (iv) are repeated until a required accuracy is reached or the difference between the parameter value of current iteration and previous iteration is zero.

In this paper, the 95% confidence interval is calculated for the transport and kinetic parameters by using the following expression [27,28]. $\widehat{p} \pm t_{N-n,\alpha/2}(s/\sqrt{N-n})\sqrt{a_{ii}}$ where $\widehat{p}$ is the point estimate for the parameter p, t is a value of Student's t distribution with $(N-n)$ degrees of freedom and $\alpha = 0.5$, i.e., 95% confidence, N is the total number of discharge data points and n is the number of fitting parameters, a_{ii} is the ith element of the principal diagonal of $(\mathbf{J}^T\mathbf{J})^{-1}$, and s is variance or deviation variable that can be calculated by $s^2 = \sum_{j=1}^{N}[(V_{cell})_j - (V_{cell})_j^*]^2$ where $(V_{cell})_j$ and $(V_{cell})_j^*$ are the predicted and experimental values of the discharge curve, respectively, at the jth point at time t.

4. Results and discussion

The parameters were estimated for the following three different cases: (1) the solid-phase diffusion coefficient alone—estimation of one parameter; (2) the solid-phase diffusion coefficient and electrolyte diffusion coefficient—estimation of two parameters; (3) the solid-phase diffusion coefficient, electrochemical rate constant at the positive electrode and electrochemical rate constant at the negative electrode—estimation of three parameters.

4.1. One parameter

Parameter estimation was carried out to compare the computation statistics for the rigorous model and efficient reformulated model. The parameter estimated was the solid-phase diffusion coefficient in the cathode; its true value is 1×10^{-15}. Table 5 shows that the rigorous model has 10 PDEs or 4800 DAEs and takes 1–2 min to complete a single iteration. It took 4 iterations to converge (using a very good initial guess) and the total time for estimating one parameter is 5–10 min using an efficient solver/good initialization. The reformulated model has 49 DAE/IDEs and takes only 60 ms to estimate a parameter in FORTRAN environment. The manual time taken between running the codes at different updated parameter values is ignored here for the purpose of stable estimation algorithm. The synthetic data (for 1C discharge) used are shown in Fig. 1 in comparison with simulated model data and the initial guess.

4.2. Two parameters

The computational run time was determined for estimating two parameters in the model equations. Fig. 2 represents the discharge curves for the synthetic experimental data, the discharge curve based on the initial guesses and the converged discharge data. Table 5 shows the computation time taken for the estimation of two parameters.

4.3. Three parameters

The computational run time was determined for estimating three parameters in the model equations. Fig. 3 represents the dis-

Table 5
Estimation of solid-phase diffusion coefficient, electrolyte diffusion coefficient and electrochemical reaction rate constants in the positive and negative electrodes

Number of parameters	Runtime for each iteration	Number of iterations
One parameter estimation	80 s (rigorous model)	4
	15 ms (reformulated model)	
Two parameters estimation	32 ms (reformulated model)	5
Three parameters estimation	35 ms (reformulated model)	2

Comparison of computational time taken by the rigorous porous electrode model and the reformulated porous electrode model.
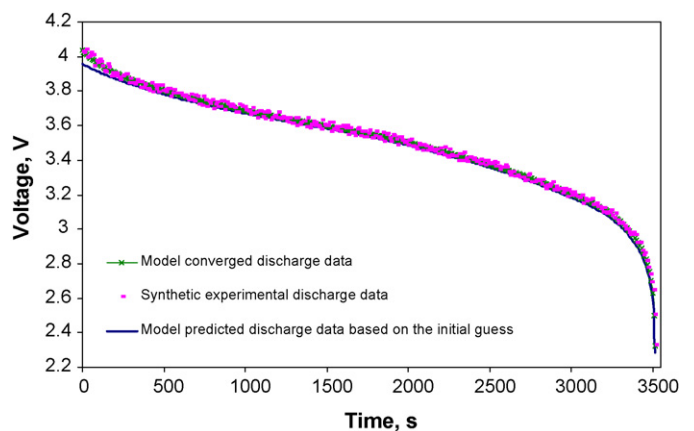
Fig. 1. Estimation of solid-phase diffusion coefficient alone. Comparison of synthetic experimental data, model predicted discharge data based on the initial guess and model converged discharge data.
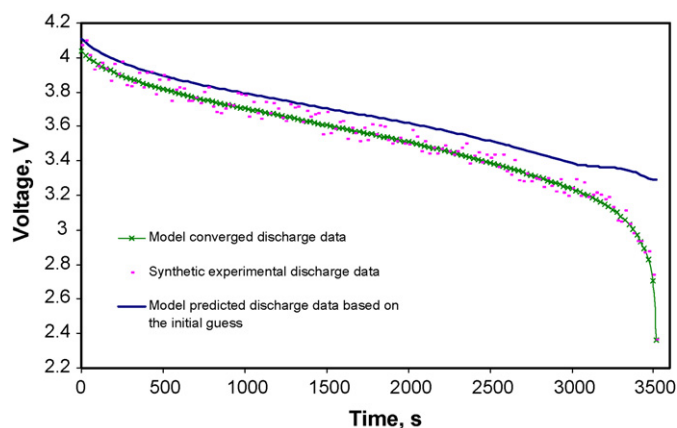
Fig. 2. Estimation of solid-phase diffusion coefficient and electrolyte diffusion coefficient. Comparison of synthetic experimental data, model predicted discharge data based on the initial guess and model converged discharge data.
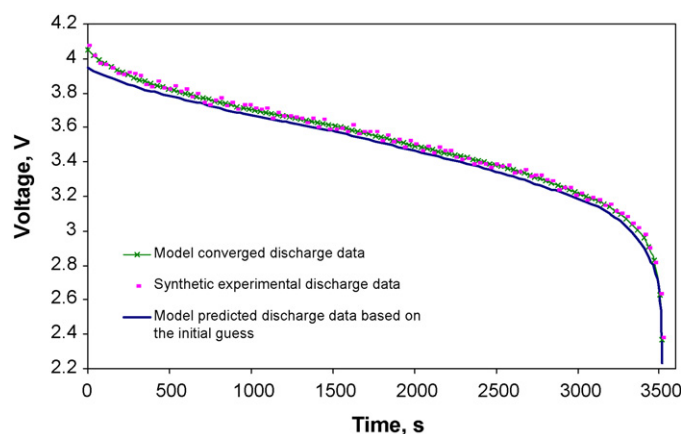

Fig. 3. Estimation of solid-phase diffusion coefficient and electrochemical rate constants in the positive and the negative electrodes. Comparison of synthetic experimental data, model predicted discharge data based on the initial guess and model converged discharge data.

Table 6

Confidence intervals for the point estimation of transport and kinetic parameters of the lithium-ion battery

Parameter	Value	95% confidence intervals
$D_{s,p}$ (m^2 s^{-1})	$1.086\,e^{-14}$	$\pm 0.307\,e^{-14}$
k_p (mol (s m^{-2})(mol m^{-3})$^{-1.5}$)	$2.360\,e^{-11}$	$\pm 0.386\,e^{-11}$
k_n (mol (s m^{-2})(mol m^{-3})$^{-1.5}$)	$5.023\,e^{-11}$	$\pm 0.019\,e^{-11}$

charge curves for the synthetic experimental data, the discharge curve based on the initial guesses and the converged discharge data. Table 5 shows the computation time taken for the estimation of three parameters.

The above three cases show that the reformulated lithium-ion battery model is very powerful and computationally efficient for parameter estimation. Table 6 shows the confidence interval for the transport and kinetic parameters that are estimated using this efficient reformulated lithium-ion battery model.

5. Conclusions

This investigation reports a real-time parameter estimation using a reformulated lithium-ion battery model. The computational benefits involved in this approach are several times better than the current state-of-the-art. These results indicate that the rigorous optimization for optimal operating conditions of lithium-ion battery model can now be evaluated using this reformulated model [29–31]. It is to be noted in this work that the estimation of parameters using lithium-ion battery models are performed only for up to 2C rate of discharge. Further reformulation of the rigorous battery model is required to enable estimation of parameters at high rates of discharge. Work in this regard is currently in progress. Future work will also involve optimization of lithium-ion battery model and other aspects related to the control of electrochemical devices.

Acknowledgements

References

[1] J. Newman, W. Tiedmann, AIChE J. 21 (1975) 25.
[2] T.F. Fuller, M. Doyle, J. Newman, J. Electrochem. Soc. 141 (1994) 982.
[3] T.F. Fuller, M. Doyle, J. Newman, J. Electrochem. Soc. 141 (1994) 1.
[4] M. Doyle, J. Newman, A.S. Gozdz, C.N. Schmutz, J.M. Tarascon, J. Electrochem. Soc. 143 (1996) 1890.
[5] K.E. Thomas, J. Newman, J. Electrochem. Soc. 150 (2003) A176.
[6] P. Arora, M. Doyle, A.S. Gozdz, R.E. White, J. Newman, J. Power Sources 88 (2000) 219.
[7] P. Ramadass, B. Haran, R.E. White, B.N. Popov, J. Power Sources 123 (2003) 230.
[8] P. Ramadass, B. Haran, P.M. Gomadam, R.E. White, B.N. Popov, J. Electrochem. Soc. 151 (2004) A196.
[9] G.G. Botte, V.R. Subramanian, R.E. White, Electrochim. Acta 45 (2000) 2595.
[10] V.R. Subramanian, J.A. Ritter, R.E. White, J. Electrochem. Soc. 148 (2001) E444.
[11] V.R. Subramanian, P. Yu, B.N. Popov, R.E. White, J. Power Sources 96 (2001) 396.
[12] V. Boovaragavan, V.R. Subramanian, Electrochem. Commun. 9 (2007) 1772.
[13] S. Santhanagopalan, Q. Guo, R.E. White, J. Electrochem. Soc. 154 (2007) A198.
[14] V.R. Subramanian, S. Devan, R.E. White, J. Power Sources 135 (2004) 361.
[15] V.R. Subramanian, R.E. White, Comput. Chem. Eng. 24 (2000) 2405.
[16] V.R. Subramanian, D. Tapriyal, R.E. White, Electrochem. Solid-State Lett. 7 (2004) A259.
[17] V. Boovaragavan, C.A. Basha, J. Appl. Electrochem. 36 (2006) 745.
[18] V. Boovaragavan, C.A. Basha, J. Power Sources 158 (2006) 710.
[19] Q. Guo, V.R. Subramanian, J.W. Weidner, R.E. White, J. Electrochem. Soc. 149 (2002) A307.
[20] V.R. Subramanian, V. Boovaragavan, K. Potukuchi, V.D. Diwakar, A. Guduru, Electrochem. Solid-State Lett. 10 (2007) A25.
[21] V.R. Subramanian, V. Boovaragavan, V.D. Diwakar, Electrochem. Solid-State Lett. 10 (2007) A225.
[22] V.R. Subramanian, V.D. Diwakar, D. Tapriyal, J. Electrochem. Soc. 152 (2005) A2002.
[23] V.R. Subramanian, V. Boovaragavan, J. Electrochem. Soc., in preparation.
[24] K.A. Smith, Electrochemical modeling, estimation, and control of lithium ion batteries, Ph.D. Thesis, The Pennsylvania State University, University Park, 2006.
[25] L. Sirovich, Q. Appl. Math. 45 (1987) 561.
[26] L. Cai, R.E. White, 213th Meeting of the Electrochemical Society, Phoenix, May 18–22, 2008.
[27] William Navidi, Statistics for Engineers and Scientists, 2nd edition, McGraw Hill, 2008.
[28] A. Constantinides, N. Mostoufi, Numerical Methods for Chemical Engineers with MATLAB Applications, Prentice Hall, 1999.
[29] V. Boovaragavan, C.A. Basha, Electrochim. Acta 51 (2005) 200.
[30] V. Boovaragavan, C.A. Basha, Chem. Eng. J. 117 (2006) 213.
[31] V. Boovaragavan, V.R. Subramanian, J. Power Sources 173 (2007) 1006.